Indian J Phys
https://doi.org/10.1007/s12648-022-02338-8

ORIGINAL PAPER

Synthesis and study the optical nonlinear properties of polypyrrole and poly(vinyl acetate) copolymer

H A Sultan[1], M Sh Hussain[2], Q M A Hassan[1]* and C A Emshary[1]

[1]Department of Physics, College of Education for Pure Sciences, University of Basrah, Basrah 61001, Iraq

[2]Department of Chemistry, College of Education for Pure Sciences, University of Basrah, Basrah 61001, Iraq

Received: 13 November 2021 / Accepted: 24 February 2022

Abstract: Poly [pyrrole-co-(vinyl acetate)] is prepared via chemical polymerization method. Obtained copolymer is characterized by Fourier transform infrared (FTIR) and thermal gravimetric analysis (TGA). The nonlinear optical properties of this copolymer are studied using the diffraction ring patterns and the Z-scan techniques using 473 nm wavelength laser beam. The total change in the copolymer index of refraction and nonlinear index of refraction are determined via the first technique while the nonlinear refractive index is determined via the second technique. The property of optical limiting of the copolymer is investigated where it is found that this medium possess optical limiting with limiting threshold of 14 mW is obtained. The diffraction rings patterns are simulated numerically via the diffraction integral of Fresnel-Kirchhoff with reasonable agreement compare to the experimental findings.

Keywords: Poly pyrrole; Polyvinyl acetate; Diffraction ring patterns; Z-scan; Optical limiting

1. Introduction

Materials having large nonlinear refractive indexes have attracted vast interest, since the word's first ruby laser developed in 1960 by T.H. Maiman, for their potential uses in variety of applications such as optical switching, optical data storage, beam flattening, self-focusing, self-defocusing, optical bi-stability, optical limiting, etc., [1–25]. Any material thought to be used in one of these applications must possess high nonlinear refractive index, third order nonlinear optical susceptibility, nonlinear absorption coefficient, etc.

To determine each one of those properties three techniques have been established viz., thermal lens, diffraction ring patterns, and the Z-scan [26–28]. The diffraction ring patterns technique can be used to calculate the total change of the medium refractive index and nonlinear refractive index while in the Z-scan the nonlinear refractive index and its sign, third order nonlinear optical susceptibility (real and imaginary parts), nonlinear absorption coefficient, etc., can be obtained.

Among the wide range of materials used in these applications are organic and inorganic materials, nematic liquid crystals, atomic vapors, chromophore substituted silica, metal nanoparticles polymers etc. The negative sign of the nonlinear refractive index indicates self- defocusing while the positive sign indicates self-focusing.

The organic materials have received the main interest of the optical society in the study of the nonlinear properties by one of these methods. We during the last three years have studied many materials that behave nonlinearly against visible continuous wave (CW), single fundamental transverse, $TM_{00,}$ mode, low power, laser beams based on the diffraction rings and Z-scan (open and closed) techniques.

The polypyrrole (PPy) is one of conducting polymers, widely studied in various applications viz., in composites of different materials, with Zeolite [29], as composites films with poly(vinylidene) fluoride, with multi-walled carbon nanotube composites layers for detection of mercury, lead and iron ions, in nanowire/graphene composite, in multi-walled carbon nanotube nanocomposites, in metacomposites, with yttrium oxide composites, in cobalt aluminum oxide nanocomposites, in one-dimensional nanostructures for shielding of electromagnetic interference, in fly ash composites, in tin oxide nanocomposites,

*Corresponding author, E-mail: qusayali64@yahoo.co.in

Published online: 21 March 2022

doped with epoxy resin nanocomposites, with polypyrrole/wood derived materials conducting composites, in biocompatible PCL/PLGAl/composites for regenerating nerves, with poly (methyl methacrylate) nanocomposites, in the synthesis of nanofibers with hierarchical structure, in nanoparticales reduced graphene oxide layer, in titanium dioxide nanospheres, as conducting nanotubes, as microactuators, as conducting polymer at various dopant concentrations, in electroactive actuator based on nanofibers, in electro-conductive fabrics, and so many other applications [30]. The nonlinear optical properties of novel PPy derivatives bearing aromatic segments was studied using the Z-scan technique [31] together with the optical nonlinearity and electrical property in multi-walled nanotube-PPy nanocomposite [32]. Poly(vinyl Acetate), PVAc, is another material that received attention such as its bond strength dependence on temperature [33], adhesive properties [34], blend films [35], fire-retardant and fire-barrier for sealant application [36], paints in artworks by Py-GC/MS [37], thermal properties [38], blend foam [39], mechanical properties improved with silica [40], improving bonding strength by controlling the amount of redox initiator [41], and thermal and mechanical properties [42].

The polypyrrole (PPy) is one of the important conducting polymers known to date. It have good electrical conductivity, good environmental stability, their ease and high flexibility in preparation, stability and good mechanical properties. Potential technological applications such as electronic and electrochromic devices [43–46], counter electrode in electrolytic capacitors, sensors [47–49], chromatographic stationary phases [50], light-weight batteries [51], and membrane separation [52].

In the present work a Poly [pyrrole-co-(vinyl acetate)] was prepared via the chemical polymerization method. The copolymer nonlinear properties were studied via the diffraction ring patterns and Z-scan methods using CW, visible 473 nm, low power single transverse, TEM_{00}, mode laser beam. The diffraction ring patterns were numerically simulated using the Fresnel-Kirchhoff integral with good agreement compare to the experimental ones.

2. Experimental details

2.1. Instrumentation

The materials used in the synthetization of the copolymer were used as received from the vendors. Pyrrole monomer (d = 0.97 g/ml), vinyl acetate monomer(d = 0.93 g/ml) and benzoyl peroxide obtained from (Merck), hydroxyl propyl cellulose, and ferric chloride obtained from (Aldrich). Pyrrole was purified by simple distillation. Fourier transform infrared (FTIR) was studied using a spectrometer model (Thermo-nicolet IR 100) while thermal gravimetric analysis was carried out using (TGA Q50 U.S.A).

2.2. Synthesis

2.2.1. Preparation of the copolymer

In a typical experiment 1 mL of pyrrole monomer was added to a stirred a100 mL of aqueous/non aqueous solution (water/toluene, 75/25% v/v) containing 5.4 g of $FeCl_3$, and 2.0 g of benzoyl peroxide. Then, after few minutes, 3 mL of (vinyl acetate) monomer was added to the stirred solution. After 6 h, the copolymer was filtered, washed several times with deionized water, finally dried at room temperature [53].

2.2.2. FTIR spectrum for copolymer

The FTIR spectrum of the prepared copolymer is shown in Fig. 1. The copolymer have a new band at (1620 cm^{-1}) which correspond to the Pyrrole/Vinyl Acetate unit. The peaks of N–H stretching vibration at (3412.76 cm^{-1}), C=O stretching vibration at (1699.58 cm^{-1}), the one characteristic of the pyrrole unit at (1542.82 cm^{-1}), C–N stretching vibration at (1306.64 cm^{-1}), C–H in-plane deformation at (1183.96 cm^{-1}), N–H in-plane deformation at (1043.97 cm^{-1}) and C–H out-of-plane deformation at (919.55 cm^{-1}).

2.2.3. Thermal gravimetric analysis of the copolymer

TGA is a method by which changes in physical and chemical properties of materials are measured as a function of temperature at constant heating rate or as a function of time at constant temperature. TGA can provide informations about physical phenomena, such as second-order transition included vaporization,sublimation, absorption and adsorption also TGA can provide information about chemical phenomena including chemisorptions, desolation (especially dehydration), decomposition and oxidation reaction. TGA thermograms of copolymer are shown in Fig. 2 demonstrates five weight losses, the first about

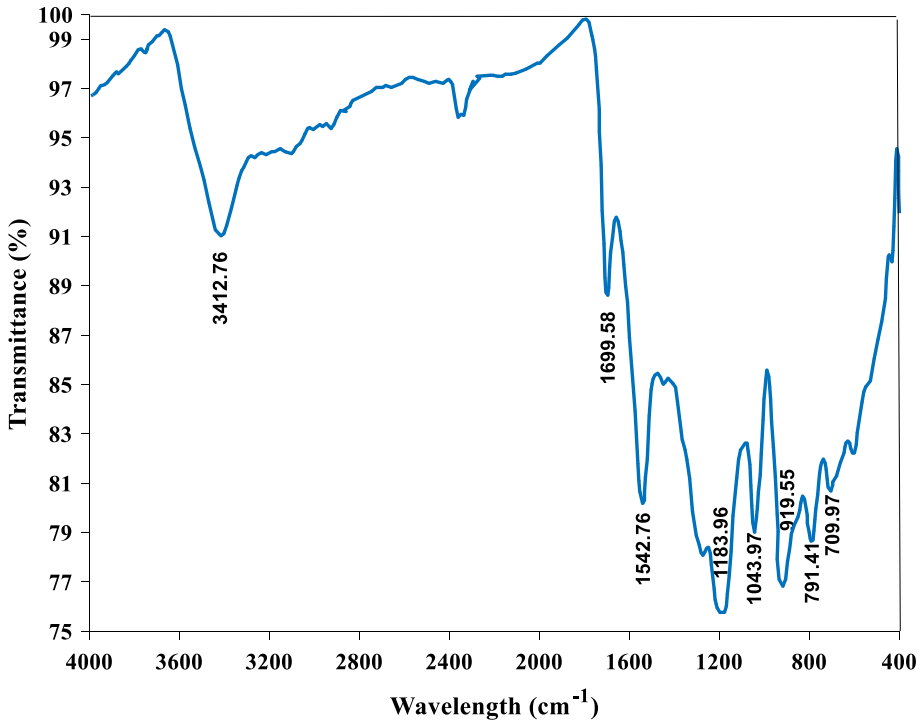

Fig. 1 FTIR spectrum of the copolymer

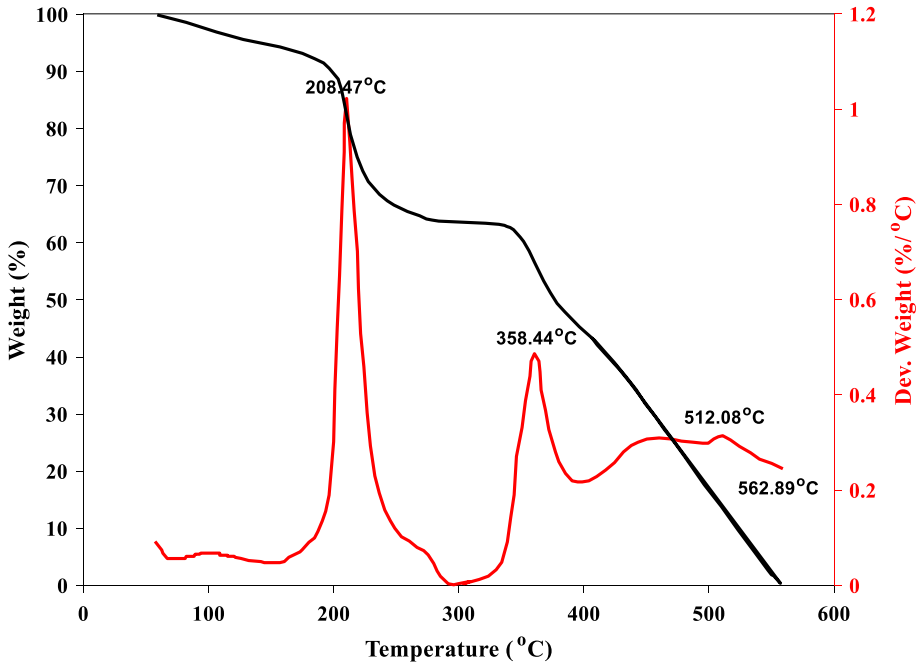

Fig. 2 TGA thermograms of the copolymer

Table 1 Thermal stability parameters from TGA thermograms of the copolymer

Optimum decomposition temp. °C			% Char.at 500 °C	Temp. of 50% Wt.loss °C	ΔE KJ/mol	Temp. range °C
Top_1	Top_2	Top_3				
208.47	358.44	512.08	15	373	52.72	313–350

(100.00 °C) corresponding to trace of H_2O, the second at (208.47 °C) corresponding to N–H, the third at (358.44 °C) corresponding to acetate, the fourth at (512.08 °C) corresponding to fragments from the copolymer backbone, and the fifth at (562.89 °C) corresponding to the residue char. The activation energy and temperature of 50% weight loss of these polymers are high. The char residues of these polymers have low char residues at 500 °C. Finally the temperature of 50% weight loss was above 240 °C. Table 1 outline all of these parameters.

2.2.4. *Spectroscopy study*

Figure 4 represents the absorbance spectrum of the copolymer using UV–visible spectrophotometer (Biotech E. M.) in the wavelength range 350–900 nm at room temperature. From Fig. 3, it is noticed that the copolymer showed a band at the wavelength λ = 265 nm, as a result of the π–π^* electronic transitions. The linear absorption coefficient, α, can be written as follows [54]:

$$\alpha = 2.303\frac{A}{d} \quad (1)$$

where d and A represent the thickness and absorbance of the sample. Using Eq. 1 and Fig. 3 where d = 0.1 cm so that α = 1.93 cm^{-1} at the wavelength 473 nm.

2.3. Experimental set-up

2.3.1. *Diffraction ring patterns*

To obtain the diffraction ring patterns the followings were used: a laser device type (SDL-473-050 T) emitting wavelength 473 nm laser beam with Gaussian intensity distribution and beam radius of 1.5 mm (at e^{-2}) as the beam leaves the laser device output coupler, a glass cell of 1 mm thick, a 5 cm focal length positive glass lens used to focus the laser beam on the sample cell, and a 30 × 30 cm semitransparent screen was used to cast the patterns of diffraction ring in the far field (85 cm to the right of the sample cell). To measure output power of laser device a power meter was used and a digital camera was used to register the resulted ring patterns.

2.3.2. *Z-scan*

The same set-up used in the previous subsection used in obtaining the Z-scan data, with a power meter covered with 2 mm diameter circular aperture replacing the screen and the sample cell was fixed on a movable stage to scan the sample cell between (− z) and (+ z) passing through the lens focal point (z = 0). This is the Z-scan closed aperture (CA). By removing the circular aperture and replaced with another positive lens to capture the entire laser beam leaving the sample cell, this is the Z-scan open aperture (OA).

2.3.3. *Optical limiting*

By fixing the sample cell position at Z-scan valley position of the CA and measuring the output power versus the input power of the laser beam, we have the optical limiting measurements setting.

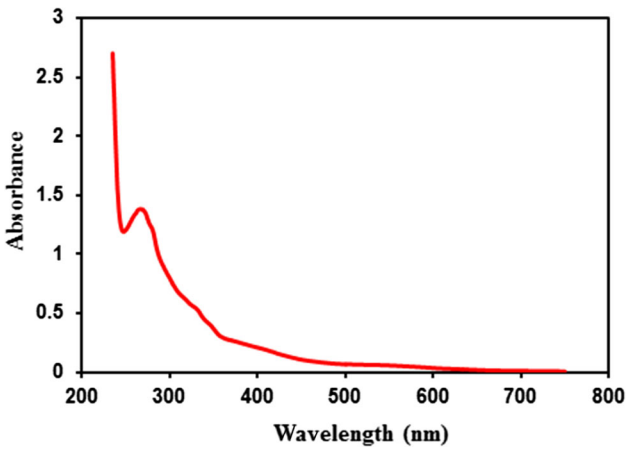

Fig. 3 The absorbance spectrum of the copolymer

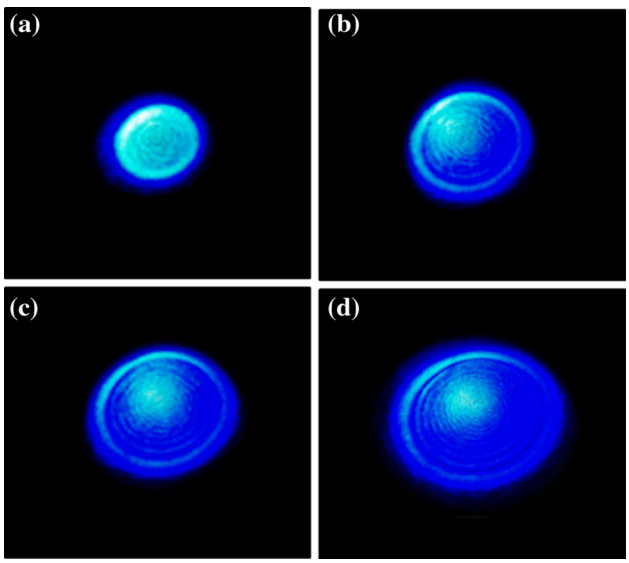

Fig. 4 Experimental diffraction ring patterns in the copolymer at input power (mW) (**a**) 19, (**b**) 32, (**c**) 49, (**d**) 66

3. Results and discussion

3.1. Diffraction ring patterns

Figure 4 shows typical far-field diffraction ring patterns evolution against input power variations falling on the copolymer cell. The input power varied slowly as (i) 19, (ii) 32, (iii) 49 and (iv) 66 mW. It can be seen that as the input power increased, the disk area that appear in Fig. 4 increased and split into ring pattern and the patterns loses symmetry in the y direction. As the area of each pattern increased, each pattern number of rings and the asymmetry increased. It can be observed that in each pattern the outer ring is the most intense relative to the inner ones as a result of self-defocusing. The asymmetries in the y-direction of the ring patterns grew in a ratio smaller compare to the x-direction as a result of thermal convection current in the y-direction which is believed to be stronger than the thermal conduction in the x-direction. The energy absorbed from the incident laser beam causes warming spatially with Gaussian distribution, so that copolymer behave like a divergent lens.

The vertical convection current act on the smoothing of the gradient of the temperature and as a result the change in the medium refractive index hence beam phase, $\Delta\varphi$, are reduced in the upper part, so that the angle made by the upper half of the patterns with the z-axis is smaller than the one made by the lower half, i.e. squeeze in the upper part occur to the ring patterns as the incident input power increased.

3.2. Z-scan

The OA Z-scan was carried out at wavelength 473 nm, and where this wavelength is away from the maximum absorption, therefore it is expected to obtain two-photon absorption or reverse saturation absorption when performing OA Z-scan using pulse laser, but when using a CW laser beam, neither of them can be obtained. In fact, this is what we got, as we got a straight horizontal line when carried out OA Z-scan, which indicates that the polymer does not have a nonlinear absorption coefficient.

Figure 5 displays the CA Z-scan results of copolymer, where it is noticed that the curve has a peak followed by a valley, which indicates the occurrence of self-defocusing, and indication that the copolymer has a negative nonlinear index of refraction. The nonlinearity displayed by the copolymer origin is thermal as a result of the use of a CW laser beam.

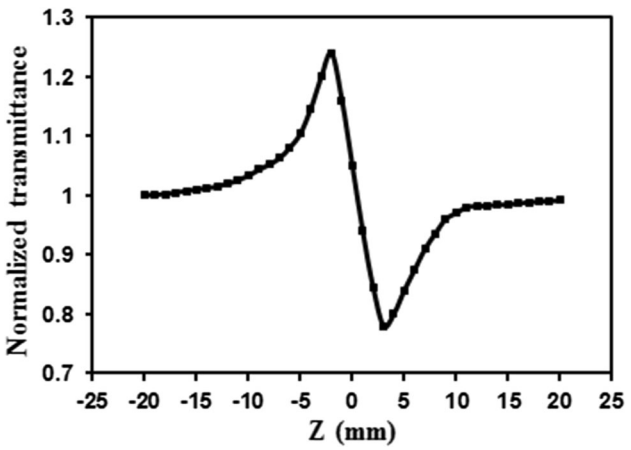

Fig. 5 CA Z-scan data for the copolymer

3.3. Optical limiting

Optical limiter is a device used to protect the optical sensors against the high intensity laser beams. The material that is used as an optical limiter must has the property that the relation between the output power and input power is

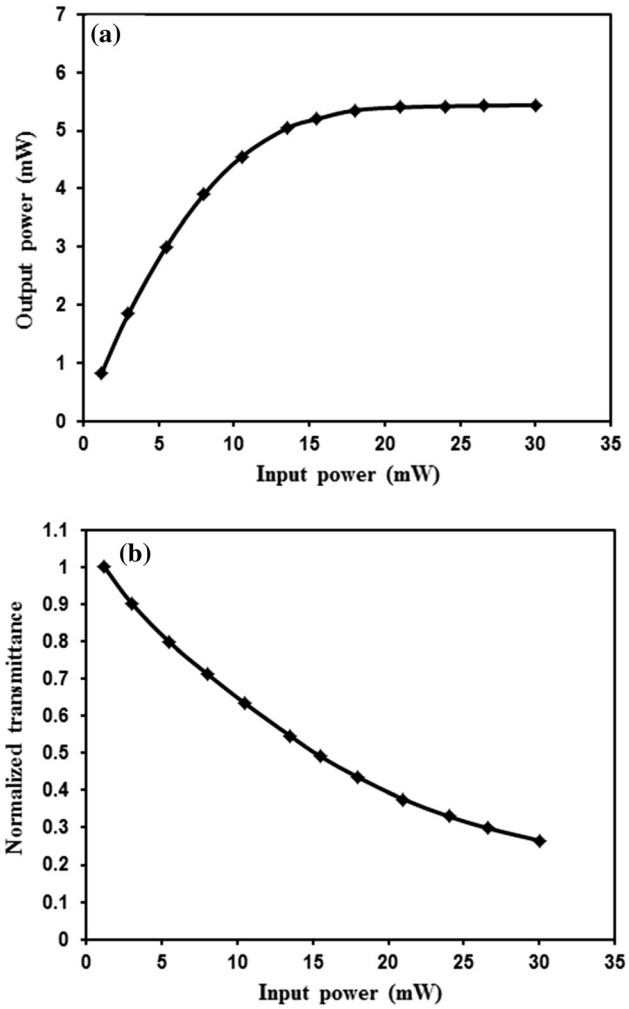

Fig. 6 (**a**) Property of optical limiting (**b**) Normalized transmittance of the copolymer

linear at low input power then the relation become nonlinear at higher input power and finally the output power must become constant as the laser beam input power increased. Figure 6a depicts the results when conducting the experiment of optical limiting, in which the output power is plotted against the input power. From Fig. 6a it can be seen that the copolymer possesses the optical limiter properties as the relation first is linear then becomes nonlinear between the output power and the input power at the low and high input power respectively, then the output power becomes constant with the increase in the input power.

3.4. Determination of the nonlinear refractive index of the copolymer due to diffraction ring pattern and Z-scan and it's optical limiting threshold

The birth of one ring as a result of the laser beam with Gaussian distribution passage in the nonlinear medium indicate a change of 2π radians of the beam phase. The total change in the beam phase for N rings, $\Delta\varphi$, is $2\pi N$ radians. $\Delta\varphi$ can be related to the total change in the medium refractive index,Δn, the sample cell thickness, d, and the propagation vector $k(=\frac{2\pi}{\lambda}$, λ is the laser beam wavelength) as follows [55]:

$$\Delta\varphi = kd\Delta n \tag{2}$$

And

$$\Delta\varphi = 2\pi N \tag{3}$$

From Eqs. 2 and 3

$$\Delta n = \frac{N\lambda}{d} \tag{4}$$

And the nonlinear index of refraction, n_2, can be obtained via the following equation

$$n_2 = \frac{\Delta n}{I} \tag{5}$$

$I = \frac{2P}{\pi\omega^2}$ is the incident intensity,P is maximum input power and ω is the beam spot size diameter at the entrance of the copolymer cell. For P = 66 mW, ω = 19.235 μm,d = 0.1 cm, λ = 473 nm, N = 12,I = 11,570 W/cm^2, so that $\Delta n = 5.676 \times 10^{-3}$ and $n_2 = 4.92 \times 10^{-7}$ cm^2/W.

According to Z-scan theory developed by Cuppo et al., the nonlinear index of refraction, n_2, is given by the following relation[56, 57]

$$n_2 = \frac{\Delta T_{p-v}\lambda}{4\pi LI} \tag{6}$$

$\Delta T_{p-v} = T_p - T_v$ is the difference between the transmittance peak, T_p, and transmittance valley, T_v, of the CA Z-scan data. From Fig. 5, and using I = 1549 W/cm^2 and Eq. 6 the value of n_2 is 0.11×10^{-7} cm^2/W.

To determine the limiting threshold value of the copolymer, a curve must be drawn between the transmittance and the input power and from this curve the value of the threshold limiting is determined, that represents the input power value for which the transmittance is reduced to half of its maximum value. Figure 6b represents the transmittance against the input power and from this Figure the value of the threshold limiting equals 14 mW.

3.5. Theoretical modeling of the diffraction ring patterns

In the present work a cw laser beam with Gaussian fundamental intensity distribution propagating along the z-direction with it's intensity vary in the x and y directions, incident on the copolymer sample cell is used. The distribution of the electric field, $U(x, y, t, z = 0)$, at the sample cell entrance usually described by the following equation [58]

$$U(x, y, t, z = 0) = \left(\frac{2P}{\pi\omega^2}\right)^{1/2} \exp\left(-\frac{x^2 + y^2}{\omega^2}\right) \exp\left(-ik\frac{x^2 + y^2}{2R}\right) \tag{7}$$

R is the of beam wave front radius. The absorption of part of the incident energy of laser beam warm the medium in the shape of Gaussian distribution. As the temperature increased, two types of currents occurs viz., conduction in the horizontal direction and convection in the vertical direction. When the two are equal, symmetric temperature gradient appears within the medium. When both are not equal asymmetries in the temperature distribution occurs. When interference occurs between each two beams emanating from the wave front of the laser beam two types of interference occurs constructive and destructive interference due to the phase difference between these beams i.e. diffraction ring pattern appears. When the vertical current overcome the horizontal one, the modulated phase of the laser beam in the upper part of the laser beam is reduced, and the diffraction ring pattern appears squeezed. This is what is observed in Fig. 4. The rise in temperature of the medium due to the absorption of

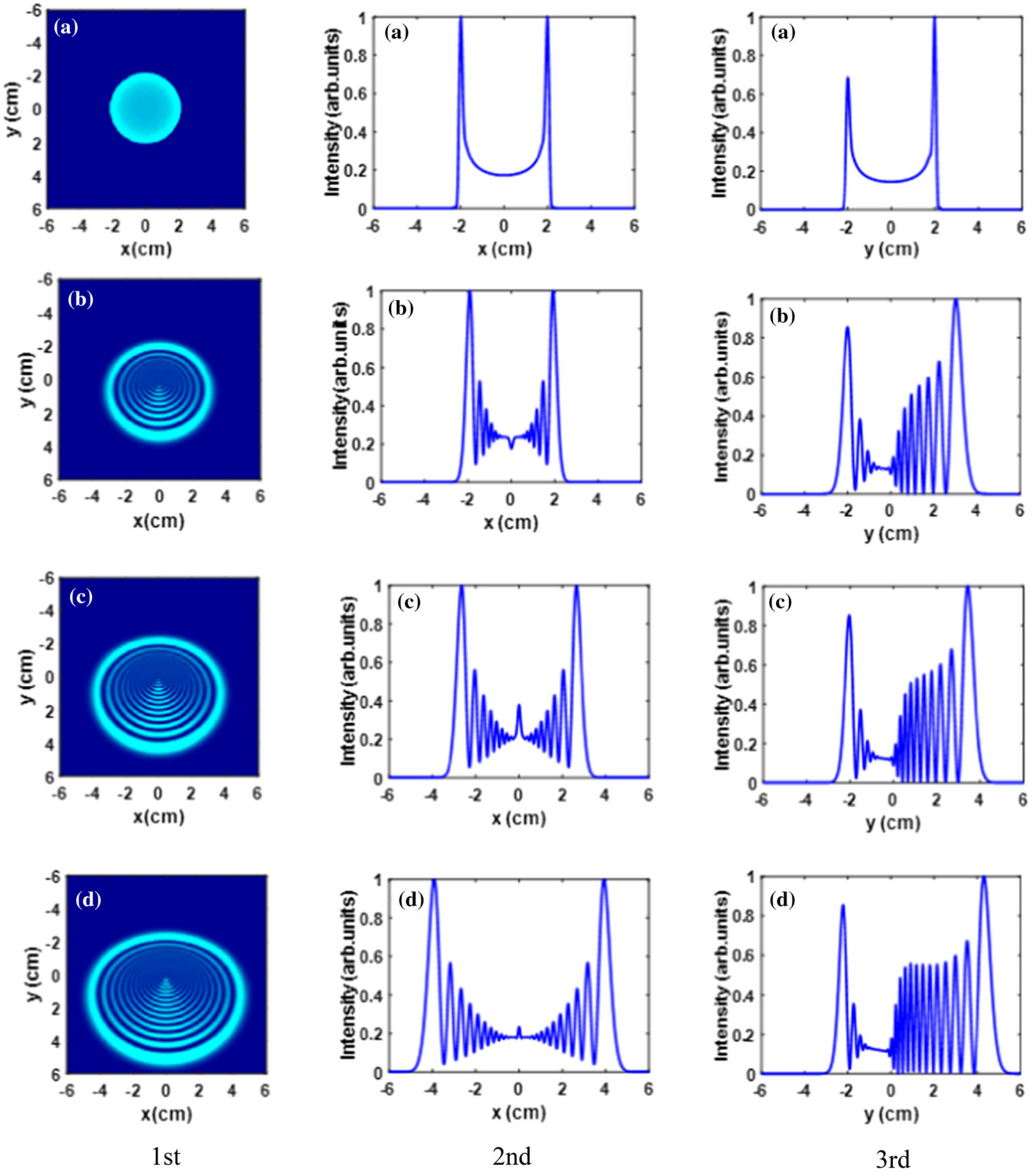

Fig. 7 Calculated patterns of diffraction rings, 1st column, 2nd and 3rd columns are the one dimensional (x) and (y) light distributions of intensity respectively at input power (mW) (**a**) 19 (**b**) 32 (**c**) 49 and (**d**) 66 in the copolymer

part of the incident energy leads to the change of medium refractive index, $n(x, y, t)$, based on the temperature rise, ΔT, and the medium thermo optic coefficient,$\frac{\mathrm{d}n}{\mathrm{d}T}$. As a result the laser beam phase shift,$\Delta\varphi(x, y, t)$, can be determined depending on the sample cell thickness,d, and the difference between $n(x, y, t)$, and the one belong to the entrance case, $n(0, 0, t)$, and the propagation wave vector, k. By taking these definitions into account the light field

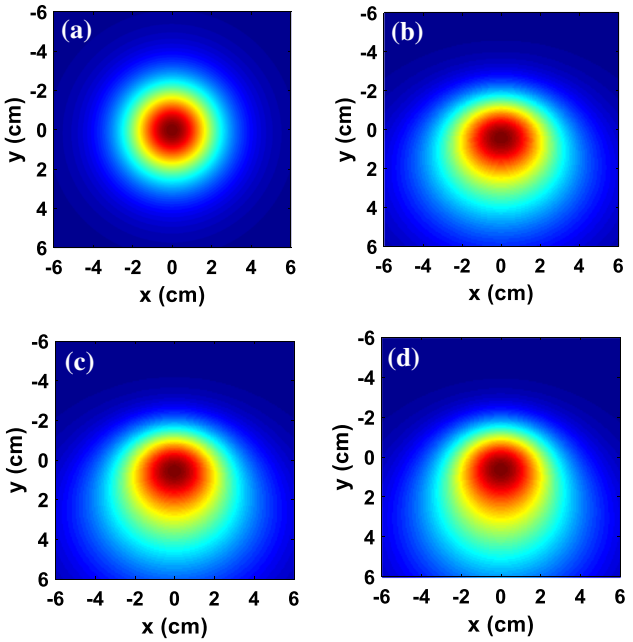

Fig. 8 The calculated laser beam phase distributions at power input (mW) (**a**) 19 (**b**) 32 (**c**) 49 and (**d**) 66 in the copolymer

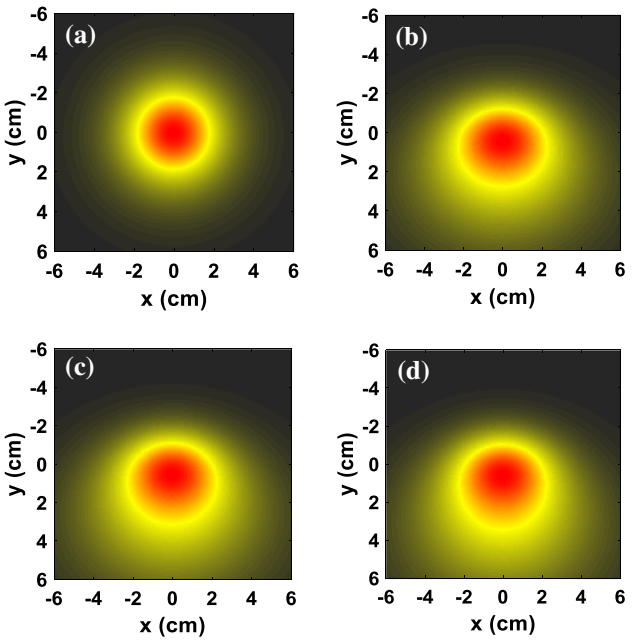

Fig. 9 The calculated temperature distributions at power input (mW) (**a**) 19 (**b**) 32 (**c**) 49 and (**d**) 66 in the copolymer

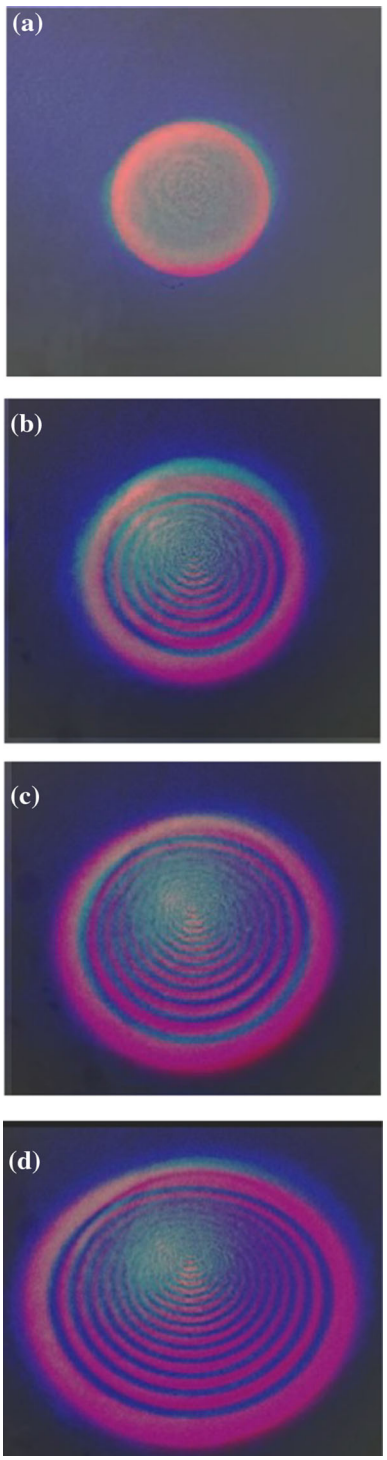

Fig. 10 Comparison of the diffraction rings patterns, experimental (blue) and the theoretical (red) at power input (mW) (**a**) 19 (**b**) 32 (**c**) 49 and (**d**) 66 in the copolymer

complex amplitude after propagation through the nonlinear medium can be written as follows:

$$U(x,y,t,z=0)=\left(\frac{2p}{\pi\omega^2}\right)^{\frac{1}{2}}\left(-\frac{\alpha d}{2}\right).\exp\left(-\mathrm{ik}\frac{x^2+y^2}{\omega^2}\right).\exp\left(-\frac{x^2+y^2}{2R}\right)\exp(i\Delta\varphi(x,y,t)) \tag{8}$$

Since the screen was located in the far-field, distance D, the spatial variables viz., x and y should be replaced by x' and y', with the use of the Fraunhofer approximation to the Fresnel-Kirchhoff diffraction integral, the distribution of light intensity on the screen can be obtained via the use of the following equation [58]

$$I(x',y',t)=\left|\left(\frac{2P}{\pi\omega^2}\right)^{\frac{1}{2}}\frac{i\pi\omega^2}{\lambda D}\exp(\mathrm{ikD})\exp\left(-\frac{\alpha d}{2}\right)\int_{-\infty}^{\infty}\mathrm{d}x\int_{-\infty}^{\infty}\mathrm{d}y.\exp\left(-\frac{x^2+y^2}{\omega^2}\right).\exp\left[i\left(-k\frac{x^2+y^2}{2R}\right)+\Delta\varphi(x,y,t)\right].\exp\left(-ik\frac{xx'+yy'}{D}\right)^2\right| \tag{9}$$

Equation (9) is solved numerically via the Mat Lab system. Figures 7, 8 and 9 are the calculated diffraction ring patterns and the one dimension (x and y) intensity distributions, spatial beam phase distributions and the spatial temperature distributions of in the copolymer at input power (mW) (i) 19, (ii) 32, (iii) 49 and (iv) 66, respectively. Figure 10 is a direct comparison of experimental (blue) against theoretical (red) diffraction ring patterns.

3.6. Comparative study

The value of the nonlinear index of refraction of the copolymer was calculated by two methods of diffraction rings and Z-scan. It can be seen when comparing the value of the nonlinear index of refraction of the copolymer computed by these two methods, that the value calculated by Z-scan is less than that the value calculated by diffraction ring pattern. This is due to the fact that the intensity used in the Z-scan method is less than the one used in the diffraction ring pattern method, and this consistent with the fact that the index of refraction depends on the intensity.

In order to know that the obtained nonlinear index of refraction value of the copolymer is high enough, we must compare it with its values for materials known to have high nonlinear optical properties, such as the materials published in previous studies [59–67], so it can be seen that the values of the nonlinear index of refraction of these materials [59–67] are less than their value for the copolymer. It should be noted here that in these studies a CW laser beam was used and the Z-scan method were used. So it can be concluded from the foregoing that the copolymer prepared in this study could be a candidate for use in electronic and optical devices applications.

4. Conclusions

Copolymer of poly pyrrole and polyvinyl acetate (PPy/PVAc) was prepared and its FTIR spectrum in the 4000–400 cm^{-1}, its thermal gravimetric analysis in the 50–550 °C range and its absorbance spectrum in the 350–900 nm were studied. The passage of visible, 473 nm laser beam in the PPy/PVAc, generated diffraction ring patterns and the Z-scan measurements so that the nonlinear index of refraction of the copolymer was determined and show optical limiting property at 473 nm wavelength. The use of Fresnel Kirchhoff diffraction integral led to the numerical simulation of the patterns of diffraction ring with reasonable agreement.

Declarations

Conflict of interest The authors declare that they have no known competing financial interests or personal relationships that could have appeared to influence the work reported in this paper.

References

[1] M F Al-Mudhaffer, A Y Al-Ahmad, Q M A Hassan and C A Emshary *Optik* **127** 1160 (2016)
[2] S Manickasundaram, P Kannan, R Kumaran, R Velu, P Ramamurthy, Q M A Hassan, P K Palanisamy, S Senthil and S S Narayanan *J. Mater. Sci. Mater. Electron.* **22** 25 (2011)
[3] S Manickasundaram, P Kannan, Q M A Hassan and P K Palanisamy *J. Mater. Sci. Mater. Electron.* **19** 1045 (2008)
[4] S Manickasundaram, P Kannan, Q M A Hassan and P K Palanisamy *Optoelec. Adv. Mat. Rap. Commun.* **2** 324 (2008)
[5] Q M A Hassan, P K Palanisamy, S Manickasundaram and P Kannan *Opt. Commun.* **267** 236 (2006)

[6] S Saghafi, M J Withford and Z Ghorauneviss *Can. J. Phys.* **84** 223 (2006)
[7] R S Elias, Q M A Hassan, C A Emshary, H A Sultan and B A Saeed *Spectroch. Acta Part A Molec. Biomol. Spec.* **223** 117297 (2019)
[8] U J Al-Hamdani, Q M A Hassan, C A Emshary, H A Sultan, A M Dhumad and A A Al-Jaber *Optik* **248** 168196 (2021)
[9] A M Dhumad, Q M A Hassan, C A Emshary, T Fahad, N A Raheem and H A Sultan *Photobiol. A Chem.* **418** 113429 (2021)
[10] Q M A Hassan and P K Palanisamy *Optik* **116** 515 (2005)
[11] Q M A Hassan and P K Palanisamy *Mod. Phys. Lett. B* **20** 623 (2006)
[12] V S Dneprovskii, A I Furtichev, V I Klimov, S Li, E V Nazvanova, D K Okorokov and U V Vandishev *Phys. Stat. Sol.* **150** 839 (1988)
[13] C A Emshary, I M Ali, Q M A Hassan and H A Sultan *Physica B* **613** 413014 (2021)
[14] Q M A Hassan and R K H Manshad *Opt. Mater.* **92** 22 (2019)
[15] C A Emshary, Q M A Hassan, H Bakr and H A Sultan *Physica B* **622** 413354 (2021)
[16] Q M A Hassan *Mod. Phys. Lett. B* **28** 1450079 (2014)
[17] Q M A Hassan, C A Emshary and H A Sultan *Phys. Scr.* **96** 095503 (2021)
[18] Q M A Hassan and R K H Manshad *Opt. Quant. Electron.* **47** 297 (2015)
[19] A M Jassem, Q M A Hassan, C A Emshary, H A Sultan, F A Almashal and W A Radhi *Phys. Scr.* **96** 025503 (2021)
[20] Q M A Hassan *Opt. Las. Technol.* **106** 366 (2018)
[21] A M Jassem, Q M A Hassan, F A Almashal, H A Sultan, A M Dhumad, C A Emshary and L T T Albaaj *Opt. Mater.* **122** 111750 (2021)
[22] H A Sultan, A M Dhumad, Q M A Hassan, T Fahad, C A Emshary and N A Raheem *Act. Part A Mole. Biomolec. Spect.* **251** 119487 (2021)
[23] Q M A Hassan and P K Palanisamy *Opt. Las. Technol.* **39** 1262 (2007)
[24] Q M A Hassan, H Bakr, C A Emshary and H A Sultan *Optik* **213** 164771 (2020)
[25] S A Ali, Q M A Hassan, C A Emshary and H A Sultan *Phys. Scr.* **95** 095814 (2020)
[26] M A Proskurnin, D S Volkov, T A Gorkova, S W Bendryshera, A P Smirnora and D A Nedosekin *J. Analy. Chem.* **70** 249 (2015)
[27] A B Villafranca and K Saravanamuttu *J. Opt. Soc. Am. B* **29** 2357 (2012)
[28] M Sheik-Bahae, A A Said, T Wei, D J Hagan and E W Van Stryland *IEEE J. Quant. Electron. QE* **26** 760 (1990)
[29] E Z M Tarmizi, H Baqiah, Z A Talib and H M Kamari *Res. Phys.* **11** 793 (2018)
[30] H Eisazadeh *World J. Chem.* **2** 67 (2007)
[31] W Zhao, Y Wang and A Wang *Mater. Sci. Appl.* **8** 774 (2017)
[32] A Bahrami, Z A Talib, E Shahriari, W M M Yanus, A Kasim and K Behzad *Int. J. Mol. Sci.* **13** 918 (2012)
[33] K Motohashi, B Tomita, H Mizumachi and H Saknguchi *Wo. Fib. Sci.* **16** 72 (1984)
[34] J V Grazulevicius, A E Barkauskas, G Buika, I Juodeikiene and D Minelga *Mater. Sci.* **9** 80 (2003)
[35] N Jelinska, M Kalnius, V Tupureina and A Dzene *Sci. J. Regavni. Mater. Sci. Appl. Chem.* **21** 55 (2010)
[36] Z Al-Hassany, A Genovese and R A Shanks *Xpr. Polym. LeH* **4** 79 (2010)
[37] S Wei, V Pintus and M Schreiner *J. Analy. Appl. Pyro.* **97** 158 (2012)
[38] T S Bachari *Bas. J. Sci. A* **33** 47 (2015)
[39] M M El-Toony and A S Al-Bayoumy *J. Chem. Eng. Proc. Tech.* **3** 1000126 (2012)
[40] R S Muwashee *Int. J. Civ. Eng. Techo.* **9** 763 (2018)
[41] Y Zhang, B Pang, S Yang, W Fang, S Yang, T-Q Yuan and R-C Sum *Materials* **11** 89 (2018)
[42] K Wang and Q Deng *Polymers* **11** 1055 (2019)
[43] H S O Chan, M Y B Teo, E Khor and C N Lim *J. Ther. Anal.* **35** 765 (1989)
[44] J Mattan, A Uusimaki, H Torvela and S Leppavuori *Makromol. Chem. Macromol. Symp.* **22** 161 (1988)
[45] A Talaie, J Y Lee, Y K Lee, J Jang, J A Romagnoli, T Taguchi and E Maeder *Th. Sol. Fil.* **363** 163 (2000)
[46] M N Rowley and R J Mortimer *Sci. Prog.* **85** 243 (2002)
[47] S B Adeloju, S J Show and G G Wallace *Anal. Chim. Acta* **281** 621 (1993)
[48] J M Slater and E J Watt *Analy. Pproc.* **26** 397 (1989)
[49] S Sukeerthi and A Q Contractor *Ind. J. Chem.* **33A** 565 (1994)
[50] H Ge, P R Teasdale and G G Wallace *J. Chromatogr* **544** 305 (1991)
[51] J Tanguy and N Mermilliod *Synth. Met.* **21** 129 (1987)
[52] A Mirmohseni, W E Price, G G Wallace and H Zhao *J. Iintell. Mater. Sys. Struc.* **4** 43 (1993)
[53] M Ghorbani and H Eisazadeh *J. Tech Sci. Press FDMP* **6** 153 (2010)
[54] K A Al-Timimy, Q M A Hassan, H A Sultan and C A Emshary *Optik* **224** 165398 (2020)
[55] K Ogusu, Y Kohtani and H Shao *Opt. Rev.* **3** 232 (1996)
[56] F L S Cuppo, A M F Neto, S L Gomez and P Palffy-Muhoray *J. Opt. Soc. Am. B* **19** 1342 (2002)
[57] K Sendhil, C Vijayan and M P Kothiyal *Opt. Las. Tech.* **38** 512 (2006)
[58] R Karimzadeh *J. Opt.* **14** 095701 (2012)
[59] R S Elias, Q M A Hassan, H A Sultan, A S Al-Asadi, B A Saeed and C A Emshary *Opt. Las. Technol.* **107** 131 (2018)
[60] A F Abdulkader, Q M A Hassan, A S Al-Asadi, H Bakr, H A Sultan and C A Emshary *Optik* **160** 100 (2018)
[61] A M Dhumad, Q M A Hassan, T Fahad, C A Emshary, N A Raheem and H A Sultan *J. Mole. Str.* **1235** 130196 (2021)
[62] D Z Mutlaq, Q M A Hassan, H A Sultan and C A Emshary *Opt. Mater.* **113** 110815 (2021)
[63] A J Kadhum, N A Hussein, Q M A Hassan, H A Sultan, A S Al-Asadi and C A Emshary *Optik* **157** 540 (2018)
[64] M H Sadr, V M Mohammadi, B Soltani, K Jamshidi-Ghaleh and S Z Mousav *Optik* **127** 6050 (2016)
[65] Z Dehghani, S Nazerdeylami, E Saievar-Iranizad and M H M Ara *J. Phys. Chem. Sol.* **72** 1008 (2011)
[66] K Kumara, T C S Shetty, S R Maidur, P S Patil and S M Dharmaprakash *Optik* **178** 384 (2019)
[67] S R Maidur and P S Patil *Optik* **190** 54 (2019)